Mechanics of Materials 216 (2026) 105626

Contents lists available at ScienceDirect

Mechanics of Materials

journal homepage: www.elsevier.com/locate/mecmat

Research paper

Bi-layer dielectric elastomer beams: Theory and applications

Karine Sacagiu [a], Silvia Monchetti [b], Roberto Brighenti [b], Noy Cohen [a,*]

[a] Department of Materials Science and Engineering, Technion - Israel Institute of Technology, Haifa 3200003, Israel

[b] Department of Civil and Environmental Engineering, University of Florence, Via di S. Marta 3, 50139 Firenze, Italy

ARTICLE INFO

Invited Editor Jean-F Molinari

Keywords:
Dielectric elastomers
Bi-layer beams
Moderate rotations theory
Actuators

ABSTRACT

Dielectric elastomers (DEs) are soft polymeric materials that deform in response to electric excitation. In this work, we investigate the behavior of bi-layer DE beams comprising layers with different electro-mechanical properties. Due to the mismatch in the properties of the layers, such beams bend when subjected to an electric field. We begin by deriving a model based on moderate rotations theory, which is an extension of linear elasticity that accounts for moderate-to-large rotations and deflections, for beams subjected to an electro-mechanical loading. The model reveals the dependency of the electro-mechanical properties of the layers on the overall response. To validate the model, we focus on free-standing beams that are subjected to two types of boundary conditions: (1) the application of an electric field across both layers and (2) imposing an electric field on one layer, while the second remains passive and serves as an elastic constraint. The model predictions show good quantitative agreement with finite element simulations. To demonstrate the practicality of using DE bi-layers, we consider the properties of commonly-employed DEs and study their performance in two types of applications — weight lifting actuators and grippers. We show that activation of a single layer enables the designs to perform a larger mechanical work. The proposed framework provides a fundamental understanding that enables efficient design of electrically activated systems, including actuators and soft robotics.

1. Introduction

Dielectric elastomers (DEs) are soft polymers that experience large deformations in response to electric excitation (Pelrine et al., 2000a; Bar-Cohen, 2001; Pelrine et al., 2000b; Madsen et al., 2016). The principle of the actuation is based on the electrically-driven thinning of a DE film that is sandwiched between two oppositely charged electrodes. Owing to the Poisson's effect, the film expands long the transverse plane.

DEs are characterized by many attractive properties such as low stiffness, high elasticity, flexibility, and fast response (Zhang et al., 2021; Yoder et al., 2024; Guo et al., 2021; Liu et al., 2015), and are therefore ideal candidates for a variety of applications. Examples include artificial muscles (Bar-Cohen, 2001; Aziz and M. Spinks, 2020), energy harvesting devices that convert mechanical energy into electrical energy (Springhetti et al., 2014; Bortot and Gei, 2015; Tutcuoglu and Majidi, 2014; Hanuhov et al., 2024; Gei et al., 2013; McKay et al., 2010), actuators capable of performing mechanical work (Kovacs and Düring, 2009; Kovacs et al., 2009; Lotz et al., 2011; Carpi and De Rossi, 2010; Cohen, 2017b; Bazaev and Cohen, 2022), soft robotics (Yang et al., 2015; Yoder et al., 2024; Xu et al., 2023), and DEs as minimum energy structures (DEMES), which are widely employed in bi-stable actuators and other devices (Khurana et al., 2021b, 2024).

In the absence of constraints, DE films experience an in-plane stretch in response to electric excitation. Recent works have shown that additional deformation modes can be achieved through the introduction of passive constraints that limit the extensibility of the DE. Specifically, DEs that are sandwiched between passive (non-responsive) elements and subjected to an electric field have been experimentally tested and modeled (Wissman et al., 2014; Franke et al., 2020; Chen et al., 2024; Khurana et al., 2024; Ahmed et al., 2014; He et al., 2017). These works show that constrained DEs can experience bending in response to electric excitation, with deflections that depend on the stiffness of the constraints and the electro-mechanical properties of the DE layer.

To enable one to better design DE based devices, various approaches have been developed over the past decades. From a continuum viewpoint, models employing variational principles which decompose the energy-density function into mechanical and electro-mechanical contributions have been proposed (Dorfmann and Ogden, 2005; Gei et al., 2014, 2013; Cao et al., 2021; Carpi and De Rossi, 2010; McMeeking et al., 2007; Suo et al., 2008; Ask et al., 2012b). Models that begin with the chain level and integrate up to the network response have also been developed (Kumar et al., 2019; Cohen et al., 2016; Brighenti et al., 2018; Cohen, 2018). These typically consider a DE film that is

* Corresponding author.
E-mail address: noyco@technion.ac.il (N. Cohen).

https://doi.org/10.1016/j.mechmat.2026.105626
Received 17 November 2025; Received in revised form 8 January 2026; Accepted 24 January 2026
Available online 3 February 2026

under simple boundary conditions, such as electrically-induced bi-axial extension. However, to fully capitalize on the promising properties of DEs in real applications, suitable numerically-based approaches that are capable of efficiently modeling this multi-physics problem under different geometries and boundary conditions are required.

The literature offers a variety of methods to tackle this problem. For example, the work of Wissler and Mazza (2005) developed a 3D finite element (FE) based framework for the inverse design of DEs by accounting for a pre-stress. Henann et al. (2013) solved the electro-mechanically coupled response of DEs by implementing a thermodynamic framework within a commercial FE code. Brighenti et al. (2018) considered the FE solution of DEs by accounting for their viscoelastic characteristics at different strain rates, while Cao et al. (2021) studied the distribution of electrostatic forces in DEs under an electric field by using the COMSOL environment. Some additional works worth mentioning are those of Croce et al. (2022), which simulated array-like DE configurations, Nejati and Mohammadi (2023), who considered the effects anisotropy in DEs aimed at harnessing the energy harvesting (EH) capabilities, and Guo et al. (2025), where tubular DE actuators were investigated.

In this work, we study the electro-mechanical response of bi-layer DE beams comprising two layers with different electro-mechanical properties. To this end, we develop a framework based on moderate rotations theory, which is an extension of linear elasticity that accounts for small strains and moderate-to-large deflections (Cohen et al., 2019; Hanuhov and Cohen, 2022), that allows to determine the overall behavior. To demonstrate the merit of the proposed model, we study two types of boundary conditions: (1) activation of the two layers in the beam and (2) activation of one layer while the other remains passive (non-responsive). Due to the mismatch between the electro-mechanical properties, the electro-mechanical load leads to bending in the two cases. The model is validated through FE simulations. To highlight the applicability of the framework, we follow by investigating the performance of bi-layer DE beams in weight lifting actuators that perform mechanical work and light grippers that respond to electric stimulus.

2. Dielectric elastomer beams

We begin by developing a model for the response of DE bi-layer beams. Consider a bi-layer beam with length L and width t comprising DE layers that are perfectly adhered to each other. The thickness, the Young's modulus, and the permittivity of the layers are denoted by $d_\bullet$, $Y_\bullet$, and $\varepsilon_\bullet$, where the subscripts $\bullet = t, b$ are used to refer to the top and the bottom layers, respectively (see Fig. 1a,b). The material points along the center-line of the beam are $\mathbf{R}(x) = x\hat{\mathbf{T}}$, where $0 \le x \le L$ and $\hat{\mathbf{T}}$ is the tangential unit vector. The bi-layer beam is subjected to an electro-mechanical loading. The loading is quasi-static and therefore we neglect viscoelastic effects (Khurana et al., 2021a).

In this work, we study two types of loadings. In the first, shown in Fig. 1a, a voltage is applied across the two layers such that the potentials φ_0 and 0 are prescribed. The potential along the interface is denoted φ_i. The second type of loading consists of the electro-mechanical activation of the top layer, while the bottom layer remains passive (Fig. 1b). In both cases, the deformed center-line of the beam, illustrated in Fig. 1c, can be written as

$$\mathbf{r}(x) = \mathbf{R}(x) + u(x)\hat{\mathbf{T}} + v(x)\hat{\mathbf{N}}, \tag{1}$$

where $\hat{\mathbf{N}}$ is a unit vector perpendicular to $\hat{\mathbf{T}}$ and $u(x)$ and $v(x)$ are the tangential and the normal displacement fields, respectively.

To determine the deformed shape of the beam, we employ moderate rotations theory, which considers beams with cross-sectional dimensions that are at least an order of magnitude smaller than the length L and assumes that (1) planar cross-sections remain planar throughout the deformation and (2) the beam experiences small strains (i.e. $s \ll 1$) and moderate-to-large rotations ($\theta^2 \ll 1$) (Cohen et al., 2019; Hanuhov and Cohen, 2022). Accordingly, the strain of the center-line can be approximated via

$$s_0(x) \approx u'(x) + \frac{1}{2}v'(x)^2, \tag{2}$$

which results in an error of $< 5\%$ for rotations of up to 30° and enables one to estimate the rotation angle $\theta(x) \approx v'(x)$ and the curvature $\kappa \approx v''(x)$ (Cohen et al., 2019; Hanuhov and Cohen, 2022). Subsequently, the strain along the cross-section of the beam can be approximated via

$$s(x, y) = s_0(x) - y v''(x), \tag{3}$$

where y is the coordinate of a material point measured from the center-line.

The stress along the direction of the beam can be written as

$$\sigma(x, y, s_E) = Y(y)\left(s_0(x) - y v''(x) - s_E(y)\right), \tag{4}$$

where $s_E(y) = \varepsilon_t \varepsilon_0 e^2/(2Y)$ is the electric field-induced strain, e is the magnitude of the electric field, and ε_t and ε_0 are the relative permittivity of the DE and the vacuum permittivity, respectively. It is emphasized that since the beam is made of two materials, the Young's modulus $Y = Y(y)$ and the electrically-induced strain $s_E = s_E(y)$ vary along the cross-section.

To determine the constitutive response of the bi-layer, we employ variational principles. A variation in the energy due to the application of forces and torques at the ends of the beam yields

$$\begin{aligned}\delta W_{ext} = {} & f_t(L)\,\delta u(L) + f_n(L)\,\delta v(L) + M(L)\,\delta v'(L) \\ & + f_t(0)\,\delta u(0) + f_n(0)\,\delta v(0) + M(0)\,\delta v'(0),\end{aligned}$$

where $f_t(x)$ and $f_n(x)$ denote the axial and the normal (shear) forces, respectively, and $M(x)$ are the moments.

A variation in the internal energy yields

$$\begin{aligned}\delta W_{int} = {} & \int_A \mathrm{d}A \int_0^L \sigma \delta s \mathrm{d}x \\ = {} & \int_A \mathrm{d}A \int_0^L E\left(s_0 - y v'' - s_E\right)\left(\delta u' + v'\delta v' - y\delta v''\right)\mathrm{d}x \\ = {} & \bar{E}\left(\left(A s_0 - \bar{Q}v'' - \bar{E}_e\right)\delta u \right. \\ & + \left(\left(A s_0 - \bar{E}_e\right)v' + \bar{Q}\left(s_0' - v''v'\right) - \bar{I}v'''\right)\delta v \\ & \left. + \left(-\bar{Q}s_0 + \bar{Q}_e + \bar{I}v''\right)\delta v'\right)\Big|_0^L \\ & - \bar{E}\int_0^L \left(\left(A s_0' - \bar{Q}v'''\right)\delta u \right. \\ & \left. + \left(\left(A s_0' - \bar{Q}v'''\right)v' + \left(A s_0 - \bar{Q}v'' - \bar{E}_e\right)v'' + \bar{Q}s_0'' - \bar{I}v''''\right)\delta v\right)\mathrm{d}x,\end{aligned} \tag{5}$$

where A is the cross-sectional area, $\bar{E} = \int_A E\mathrm{d}A/A$ is the effective Young's modulus, $\bar{Q} = \int_A Ey\mathrm{d}A/\bar{E}$ is the normalized first moment of inertia, and $\bar{I} = \int Ey^2\mathrm{d}A/\bar{E}$ is the normalized second moment of inertia. In terms of the electrically-induced strain, we define $\bar{E}_e = \int_A E s_E \mathrm{d}A/\bar{E}$ and $\bar{Q}_e = \int_A E y s_E \mathrm{d}A/\bar{E}$.

For any variation in δu, δv, and $\delta v'$, the relation $\delta W_{ext} = \delta W_{int}$ must hold. Accordingly, we collect like terms and obtain

$$A s_0' - \bar{Q}v''' = \left(A s_0 - \bar{Q}v''\right)' = 0, \tag{6}$$

and

$$\left(A s_0 - \bar{Q}v'' - \bar{E}_e\right)v'' + \left(\frac{\bar{Q}^2}{A} - \bar{I}\right)v'''' = 0, \tag{7}$$

where in passing the relation $s_0'' = \bar{Q}v''''/A$ is employed.

Next, we can write

$$\mp\eta\left(\frac{\xi}{L}\right)^2 v'' + v'''' = 0, \tag{8}$$

where

$$\eta = \frac{A^2L^2}{A\bar{I} - \bar{Q}^2} > 0, \tag{9}$$

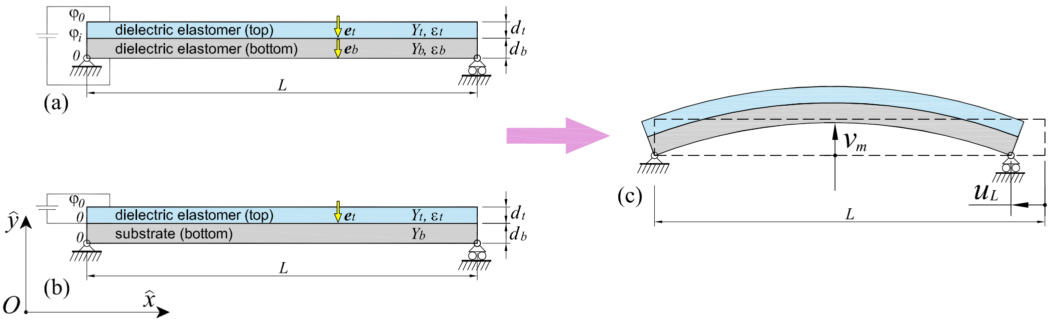

Fig. 1. Electric-mechanical loading of a bi-layer DE beam: (a) activation of the two layers, (b) activation of one layer while the other remains passive, and (c) the deformed shape.

is a constant that depends on the material properties and the geometry of the strut and

$$\pm\xi^2 = s_0 - \frac{\bar{Q}}{A}v'' - \frac{\bar{E}_e}{A}, \tag{10}$$

is proportional to the applied force, as will be shown in the subsequent equations. The plus and the minus signs in the above equations account for tension and compression, respectively.

Substitution of Eq. (10) into Eq. (2) yields the tangential displacement field,

$$u(x) = \left(\pm\xi^2 + \frac{\bar{E}_e}{A}\right)x + \frac{\bar{Q}}{A}v' - \frac{1}{2}\int v'(x)^2 \mathrm{d}x + c, \tag{11}$$

where c is an integration constant determined from the boundary conditions on the tangential displacement.

The tangential and normal forces at the ends are

$$f_t(0) = \mp\bar{E}A\xi^2;\;\; f_t(L) = \pm\bar{E}A\xi^2, \tag{12}$$

and

$$f_n(0) = \bar{E}A\left(\mp\xi^2 v' + \frac{L^2}{\eta}v'''\right);\;\; f_n(L) = \bar{E}A\left(\pm\xi^2 v' - \frac{L^2}{\eta}v'''\right), \tag{13}$$

respectively. The moments acting on the two ends of the beam are

$$M(0) = \bar{E}\left(\left(\pm\xi^2 + \frac{\bar{E}_e}{A}\right)\bar{Q} - \bar{Q}_e - \frac{AL^2}{\eta}v''\right);$$
$$M(L) = \bar{E}\left(\left(\mp\xi^2 - \frac{\bar{E}_e}{A}\right)\bar{Q} + \bar{Q}_e + \frac{AL^2}{\eta}v''\right). \tag{14}$$

To determine the response of a DE beam subjected to one of the two electro-mechanical loadings described in Fig. 1, we must prescribe mechanical and electrical boundary conditions. In terms of mechanics, the boundary conditions are given in terms of displacements or forces and moments at the ends (Eqs. (8), (11), (12), (13), and (14)). From an electrical viewpoint, one can apply a potential difference and accordingly determine the electric field, as shown in the following sub-section.

2.1. The electric field across the layers

In the case of two layers characterized by different permittivities ε_t and ε_b, as shown in Fig. 1a, the electric field acting on each layer differs. To determine e_t and e_b, we assume that the electric fields are parallel to the beam thickness. Due to the continuity of the electric displacement field, $\varepsilon_t e_t = \varepsilon_b e_b$ and the voltage across the two layers is $\varphi_0 = e_t d_t + e_b d_b$. These two relations enable to determine the electric fields

$$e_t = \frac{\varepsilon_b}{\varepsilon_b d_t + \varepsilon_t d_b}\varphi_0;\;\; e_b = \frac{\varepsilon_t}{\varepsilon_b d_t + \varepsilon_t d_b}\varphi_0. \tag{15}$$

One can also compute the potential along the interface

$$\varphi_i = \frac{\varepsilon_t d_b}{\varepsilon_b d_t + \varepsilon_t d_b}\varphi_0. \tag{16}$$

Table 1
The electro-mechanical properties of the dielectric elastomers.

Material	Young's modulus Y	Relative permittivity ε
1	0.2 MPa	4.7
2	0.4 MPa	4.7
3	0.2 MPa	4
4	0.4 MPa	4

In the second case depicted in 1b, the top layer is subjected to the electric field $e_t = \varphi_0/d_t$ and the bottom layer is passive.

3. Electric excitation of free standing bi-layer beams

To study the response of bi-layer DE beams, we consider free standing bi-layer beams under two types of boundary conditions (as described in Fig. 1): (1) application of a voltage across the two layers of the beam and (2) activation of the top layer, while the bottom DE remains passive and serves as an elastic constraint.

Following the proposed framework, we begin by deriving the expressions for the displacement field of the beam. Consider a free-standing bi-layer beam that experiences bending to an electro-mechanical loading. To prevent translation and rotation, we set $u(0) = v(0) = v(L) = 0$ and write the boundary conditions

$$f_t(L) = 0;\;\; M(0) = M(L) = 0. \tag{17}$$

According to Eq. (12), the absence of a tangential force yields $\xi = 0$. Accordingly, Eqs. (8) and (11) can be solved to determine the normal and tangential displacements

$$v(\bar{x}) = \frac{\eta\left(A\bar{Q}_e - \bar{Q}\bar{E}_e\right)}{2A^2}(1-\bar{x})\bar{x}, \tag{18}$$

and

$$u(\bar{x}) = \left(\frac{\bar{E}_e}{A}L - \frac{8v_m}{L}\left(\frac{\bar{Q}}{A} + v_m\right)\right)\bar{x} + \frac{16v_m^2}{3L}(3-2\bar{x})\bar{x}^2, \tag{19}$$

respectively, where $0 \le \bar{x} = x/L \le 1$ and $v_m = v(x = L/2)$. For convenience, we define the tangential displacement $u_L = u(\bar{x} = 1)$, which measures the change in the distance between the two ends of the beam. We point out that based on Eq. (18), the direction of bending is determined by the geometry and the electro-mechanical properties of the layers via the quantity $A\bar{Q}_e - \bar{Q}\bar{E}_e$.

To simulate the behavior of the beams, we set the length $L = 0.1$ m and the thicknesses of the two layers $d_t = d_b = 0.1$ mm. The top layer assumes the typical properties of commonly used DEs (such as, for example, adhesive dielectric VHB 4910 (Bozlar et al., 2012; Cohen et al., 2017; Kofod et al., 2003)) and the bottom layer assumes three typical stiffnesses and relative permittivities, as listed in Table 1.

To validate the model, we compare its predictions to FE simulations, which follow the formulation of Dorfmann and Ogden (2005) and assume the neo-Hookean form for the DEs. The FE algorithm is

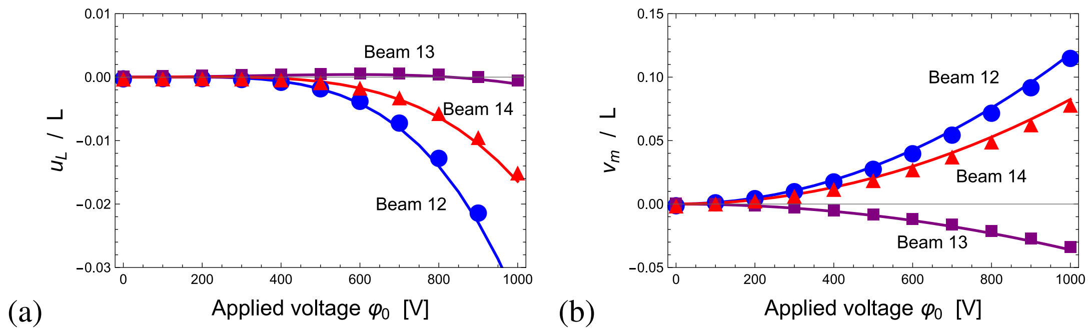

Fig. 2. (a) The normalized tangential displacement u_L/L and (b) the normalized normal displacement v_m/L as a function of the applied voltage φ_0 for free standing bi-layer beams with the activation of two layers comprising materials 12, 13, and 14. The marks denote the finite element simulations and the continuous curves are the predictions of the proposed model.

based on previous works (Dorfmann and Ogden, 2023; Ask et al., 2012a; Brighenti et al., 2018) and is summarized in the supplemental information for convenience.

3.1. Activation of a bi-layer

First, we consider the application of an electric field to two layers with incompatible electro-mechanical properties (see Fig. 1a). In a homogeneous beam with $\varepsilon_t = \varepsilon_b = \varepsilon$, $Y_t = Y_b = Y$, and an overall thickness d it can be shown that there is no bending and the axial strain is $s = \varepsilon e^2/(2Y)$. This classical result has been observed in experiments (Pelrine et al., 2000b; Hajiesmaili and Clarke, 2021).

To investigate the role of the stiffness and the relative permittivity of the layers on the overall electro-mechanical response, we consider three bi-layer beams with a top layer made of material 1 (VHB 4910). The bottom layer of the three beams are set as materials 2, 3, and 4, respectively (see Table 1). Henceforth, we refer to the beams as beam 12, beam 13, and beam 14, such that the first and the second indices denote the materials for the top and the bottom layers, respectively.

Figs. 2a and 2b plot the normalized tangential displacement u_L/L and the normalized normal displacement v_m/L as a function of the applied voltage φ_0, respectively. The finite element results are denoted by the marks and the continuous curves correspond to the model predictions. We point out that due to the very high slenderness of the beam, the use of elements with an aspect ratio close to one is required to obtain reliable results from the FE simulations. In order to limit the FE computational cost, the numerical analyses was conducted with six elements along the beam thickness. This limited number of elements is one of the causes for the error observed between the FE and the theoretical model for low voltage values.

We point out that the tangential displacements are significantly smaller than the normal displacements, i.e. $|u_L| \ll |v_m|$. Furthermore, as shown in Eq. (18), the direction of bending is determined by the quantity $\varepsilon_b Y_b - \varepsilon_t Y_t$. Since $\varepsilon_2 Y_2 - \varepsilon_1 Y_1 > 0$ and $\varepsilon_4 Y_4 - \varepsilon_1 Y_1 > 0$ beams 12 and 14 bend upwards, whereas in beam 13 $\varepsilon_3 Y_3 - \varepsilon_1 Y_1 < 0$ and a downwards bending is observed.

3.2. Activation of a single layer

Next, we consider a bi-layer beam in which only the top layer is activated, as shown in Fig. 1b. The normal and tangential displacements $v_m = v(x = L/2)$ and $u_L = u(\bar{x} = 1)$ are obtained by substituting the electric fields $e_t = \varphi_0/d_t$ and $e_b = 0$ into Eqs. (18) and (19), respectively. As in the previous sub-section, we consider the properties of VHB 4910 for the top (active) layer (material 1 in Table 1) and vary the stiffness of the bottom (passive) layer.

We begin by investigating the influence of the stiffness of the bottom layer on the normalized tangential displacement u_L/L and the normalized normal displacement v_m/L in Figs. 3a and b, respectively.

Table 2
The electro-mechanical properties of representative DEs.

Material	Young's modulus Y (MPa)	Relative permittivity ε
VHB 4910	0.22	4.7
Elastosil RT 625	1.025	2.7
Fluorosilicone 730	0.5	6.9

In the limit $Y_b/Y_t \to 0$, i.e. an extremely compliant bottom layer, we find that $v(\bar{x}) = 0$ and $u_L/L = \varepsilon e_t^2/\left(2Y_t\right) > 0$. This result corresponds to the deformation of a homogeneous DE, since the bottom layer does not constrain the electrically-induced strain. In the case of an extremely stiff bottom layer ($Y_b/Y_t \to \infty$), the electric fields do not generate sufficient force to cause any deformation and therefore $v(\bar{x}) = 0$ and $u(\bar{x}) = 0$. A maximum value is obtained when the stiffness of the passive constraining layer matches that of the active layer, i.e. $Y_b/Y_t = 1$. It is also interesting to note that while the deflection is always upwards, the tangential displacement $u_L/L > 0$ for a small range of values in the vicinity of $Y_b/Y_t \to 0$.

As opposed to the previous case, in which both layers were subjected to electric excitation, the magnitude of the tangential displacement here is larger than the deflection (i.e. $|u_L| > |v_m|$) for a wide range of stiffness ratios. This phenomenon can be explained as follows: the actuation of the bottom layer leads to its stretching, which aims to extend the overall distance between the two ends of the beam. The negative displacement u_L is due to the bending effect. If the bottom layer is non-responsive, i.e. there are no forces that work towards its stretching, the electrically-induced bending leads to a sharper decrease in u_L.

To validate the model under these boundary conditions, we consider the stiffness ratios $Y_b/Y_t = 1, 10$, and 50 and compare the predictions to the results from FE simulations. Figs. 4a and 4b depict the normalized tangential displacement u_L/L and the normalized normal displacement v_m/L as a function of the applied voltage φ_0, respectively. The model predictions (continuous curves) agree with the FE simulations (marks).

4. Applications

To demonstrate the merit of the proposed framework, in this section we investigate the performance of DE bi-layer beams in two applications: (1) a weight lifting actuator and (2) soft grippers. To this end, we consider the properties of three widely used DEs, namely VHB 4910 (Kofod et al., 2003; Bozlar et al., 2012; Bazaev and Cohen, 2022), Elastosil RT 625 (Kofod and Sommer-Larsen, 2005; Cohen et al., 2017; Cohen, 2018), and Fluorosilicone 730 (Kornbluh and Pelrine, 2008; Shmuel, 2015). The electro-mechanical properties are summarized in Table 2. In addition, we set the length of the DE beams $L = 0.1$ m, the thickness of the two layers $d_t = d_b = 0.1$ mm, and the width $t = 0.2$ mm.

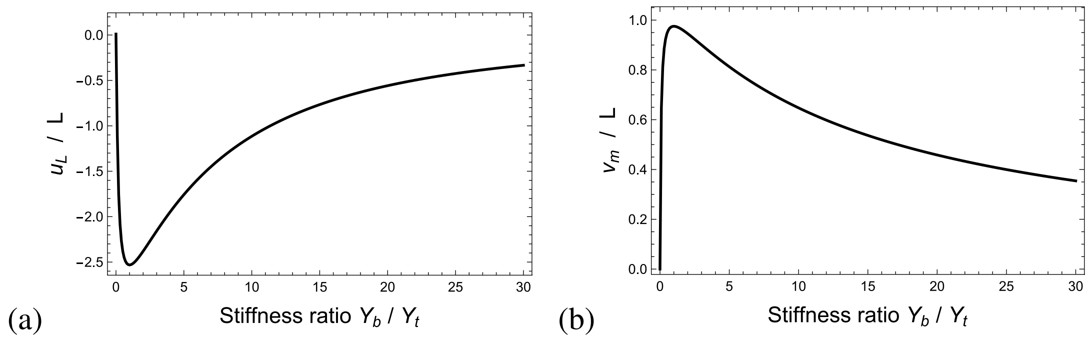

Fig. 3. (a) The normalized tangential displacement u_L/L and (b) the normalized normal displacement v_m/L as a function of the stiffness ratios Y_b/Y_t for a bi-layer with one passive layer under an applied voltage $\varphi_0 = 1\,\text{kV}$.

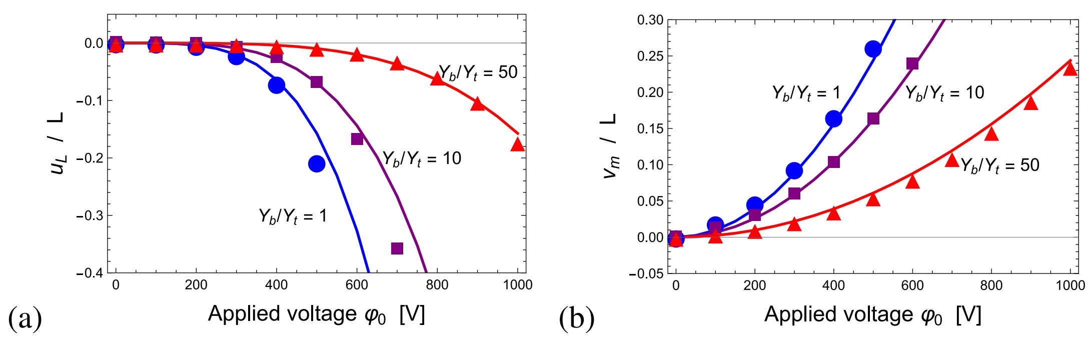

Fig. 4. (a) The normalized tangential displacement u_L/L and (b) the normalized normal displacement v_m/L as a function of the applied voltage φ_0 for a bi-layer with one passive layer and the stiffness ratios $Y_b/Y_t = 1, 10$, and 50. The marks denote the finite element simulations and the continuous curves are the predictions of the proposed model.

4.1. Weight lifting DE actuators

Homogeneous DE films, which expand along the direction perpendicular to the electric field, have been used in the design of actuators that are capable of lifting loads (Kovacs and Düring, 2009; Liu et al., 2017; Kovacs et al., 2009; Cohen, 2017a; Lotz et al., 2011; Tutcuoglu and Majidi, 2014). Typically, the actuators comprise stacked DEs that are connected in parallel or in series and activated separately in order to perform significant mechanical work. As opposed to the transverse expansion of homogeneous DE films, DE bi-layers bend and therefore contract along the longitudinal direction. As previously shown, the bending amplitude depends on the mismatch in the electro-mechanical properties between the two layers. As opposed to the standard designs, in this work we propose an actuator that can perform mechanical work along the direction perpendicular to the electric field. As illustrated in Fig. 5, consider a weight that is connected to the end of a pinned beam. In the absence of an electric field, the beam stretches due to the weight. Once an electric field is applied, the beam bends such that the distance between its two ends decreases, thereby lifting the weights. We note that DEs are typically thin to generate large electric fields and meaningful deformations, and therefore the applied weight on a single beam must be small. To overcome this, a few actuators can be connected in parallel, as shown in Fig. 5(right).

The merit of this type of actuator can be demonstrated through the proposed framework. In this case, the beam is subjected to a tensile dead-load W such that

$$f_t(L) = \bar{E}A\xi^2 = W. \tag{20}$$

Accordingly, one can determine $\xi = \sqrt{W/\bar{E}A}$. The remaining boundary conditions are $u(0) = v(0) = 0$, $f_n(L) = 0$, and $M(0) = M(L) = 0$. In the following, we choose the material VHB 4910 for the upper layer and the bottom layer is made of Elastosil 625 or Fluorosilicone 730 (see properties in Table 2).

Fig. 6 plots the normalized lifting height u_L/L of a $W = 0.05\,\text{mN}$ (or 5 mg) weight as a function of the applied voltage φ_0 in bi-layer DE beams under the activation of a single layer and the activation of the two layers. The bottom layers considered in Fig. 6a and b are Elastosil 625 and Fluorosilicone 730, respectively.

Comparison of the two actuation methods reveals that the activation of a single layer enables one to achieve higher lifting (or greater mechanical work). This phenomenon highlights the advantages of single layer activation and can be explained as follows: the electric forces applied on a DE film aim to extend along the perpendicular direction. Activation of a single layer that is constrained by a passive film has less "stretching" mechanisms, and thus a higher degree of bending is achieved. In addition, the application of a voltage across a single layer leads to higher electric fields, which enhance the overall performance of the actuator.

Fig. 6a and b reveal that the mismatch between the properties of the two layers is also a significant factor in determining the performance of the actuator. Specifically, beams with a passive Elastosil layer are capable of lifting the same weight under lower voltages when only one layer is activated. Here, the stiffness of the Elastosil limits the deformation due to the weight in the absence of loading, and therefore under stretch larger displacements u_L can be obtained. If both layers are activated, Fluorosilicone performs better due to its higher relative permittivity.

It is underscored that the weight which can be carried by the system can be increased through the connection of several actuators in parallel, as demonstrated in Fig. 5. Similar concepts were employed in previous works (Duduta et al., 2016; Xiao et al., 2020), where DE layers were connected in parallel and a blocked force on the order of $< 2.5\,\text{mN}$ was measured under $\sim 2\,\text{kV}$. Other works stacked DE films in series and

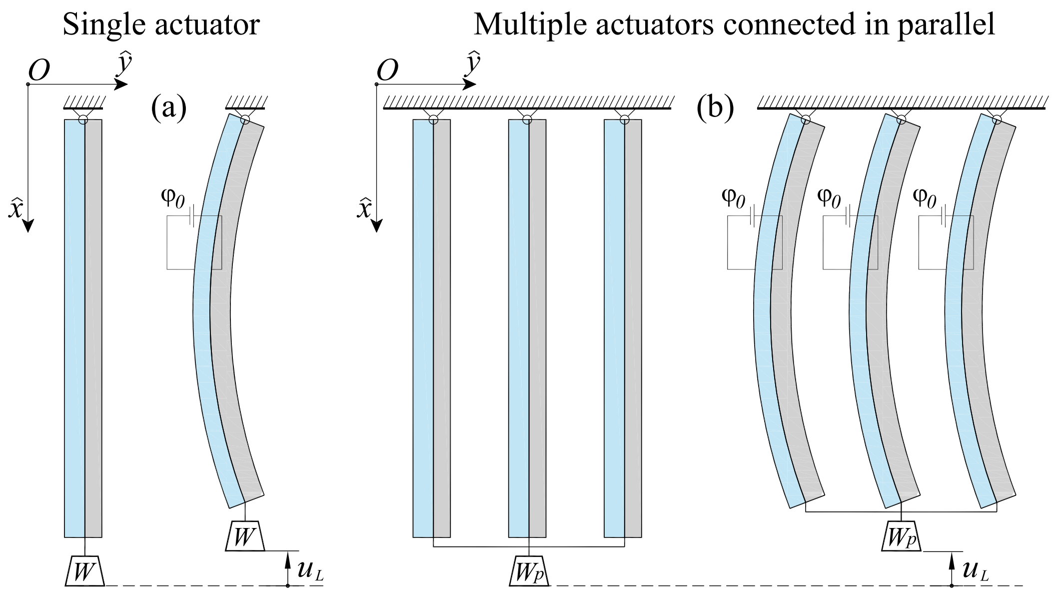

Fig. 5. Actuator design for lifting weight via electric excitation: (left) single actuator and (right) multiple actuators connected in parallel capable of lifting heavier loads.

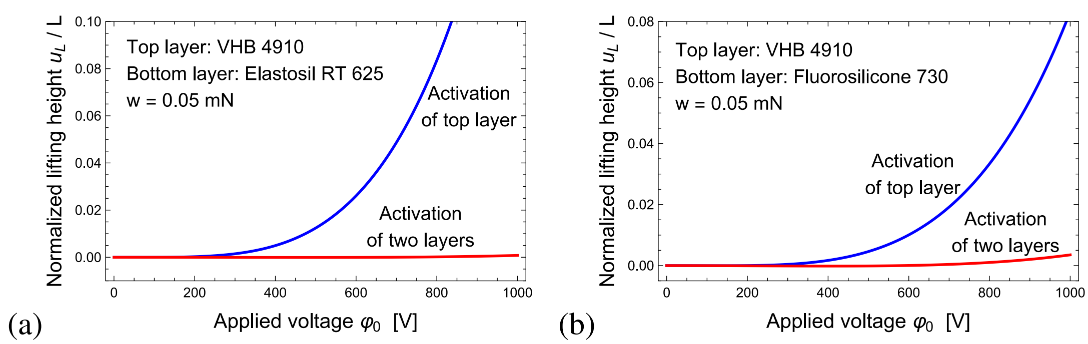

Fig. 6. The normalized lifting height u_L/L of a $W = 0.05\,\mathrm{mN}$ (5 mg) weight as a function of the applied voltage φ_0 for a bi-layer beam with activation of a single layer and two layers. The top layer is made of VHB 4910 and the bottom layer is (a) Elastosil RT 625 and (b) Fluorosilicone 730.

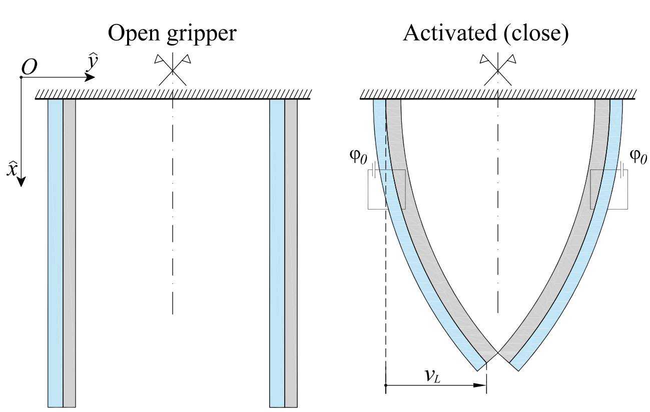

Fig. 7. A gripper comprising bi-layer DE beams.

applied the same potential difference to each film (Kovacs et al., 2009). As opposed to the current approach, in which work is achieved by the bending of the bi-layer, the lifting in a stacked DE set-up is done along the thickness. The work of Kovacs et al. (2009) demonstrated the lifting of $> 2\,\mathrm{kg}$ (or $> 20\,\mathrm{N}$) with approximately 400 DE layers with strains of $\sim$ 10%. The work that can be done along the thickness is larger than that which can be done along the thickness. Specifically, based on our design a weight of $0.05\,\mathrm{mN}$ was lifted with a single layer at $\sim 1\,\mathrm{kV}$ with a strain of $\sim$ 10%. Therefore, 400 bi-layer beams connected in parallel can lift $\sim 20\,\mathrm{mN}$. This drawback stems from the lifting mechanism — the proposed design is based on bending while the former relies on compression of thin films. As a result, the displacement of all of the bi-layer beams in the parallel bending mechanism is the same, whereas in the stacked DE set-up the displacements accumulate and are proportional to the number of DE layers (Cohen, 2017a; Kovacs et al., 2009).

From a practical viewpoint, one of the main limitations of DE-based actuators is electric breakdown. Recent works showed that pre-stretching can be used to enhance the electric fields and delay electric breakdown (Kofod, 2008; Su et al., 2019; Li et al., 2011; Kumar et al., 2019; Kumar and Sarangi, 2020; Zurlo et al., 2017). In the context of the proposed bi-layer actuators, pre-stretching of the layers can induce an initial curvature due to the mismatch between the mechanical properties of the layers, which must be accounted for.

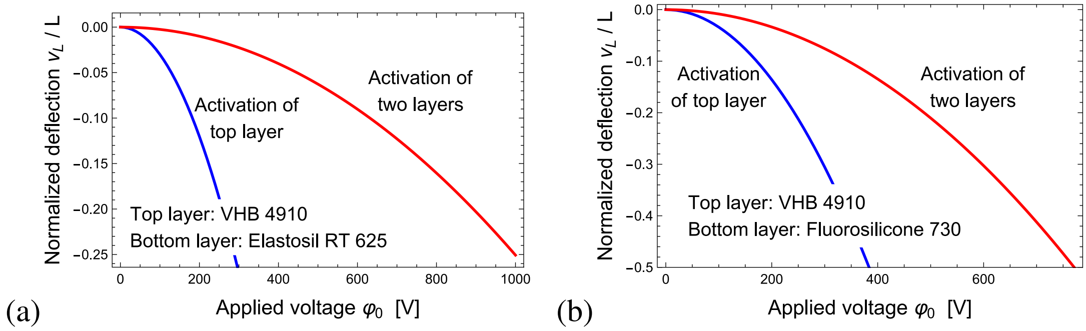

Fig. 8. The normalized deflection v_L/L as a function of the applied voltage φ_0 for a bi-layer beam with activation of a single layer and two layers. The top layer is made of VHB 4910 and the bottom layer is (a) Elastosil RT 625 and (b) Fluorosilicone 730. of the free layers t.

4.2. Grippers

Next, we examine the use of bi-layer DE beams in soft grippers, as shown in Fig. 7. Thanks to their lightweight, fast response, and efficiency, the use of DEs in grippers and soft robotics applications to grab and lift objects (Shian et al., 2015; Thongking et al., 2021; Wang et al., 2022; Jamali et al., 2024; Zhang et al., 2025).

To explore the performance of the gripper, we employ our framework. The DE beam is fixed at the top and does not experience any axial forces (see Fig. 7). Therefore, $\xi = 0$ and we require that $u(0) = v(0) = v'(0) = 0$, $f_n(L) = 0$, and $M(L) = 0$. For convenience, we denote the deflection at the end of the beam by $v_L = v(L)$.

Since the gripper must close under voltage, the direction of bending of the gripper arms is important. In the case of single layer activation, the beam bends towards the passive layer such that the actuated DE experiences stretch. In the activation of the two layers, the bending direction is determined by the relation $\varepsilon_t Y_t - \varepsilon_b Y_b$ - if this difference is positive, the beam bends towards the top layer.

Fig. 8a and b depict the normalized deflection v_L/L as a function of the applied voltage φ_0 for two types of activation loadings in bi-layers with a top layer that is made of VHB 4910 and bottom layers from Elastosil RT 625 and Fluorosilicone 730, respectively. Note that in both cases, $\varepsilon_t Y_t - \varepsilon_b Y_b < 0$ and therefore the bending is towards the bottom layer. We find that activation of a single layer leads to larger deflections at lower voltages due to the absence of "stretching mechanisms" in the passive layer. In addition, comparison of the two materials we examined for the bottom layer reveals that the Fluorosilicone leads to higher deflections due to its compliance.

5. Conclusions

In this work, we develop a framework for perfectly adhered bi-layer DE beams that bend in response to an electro-mechanical loading due to a mismatch in electro-mechanical properties of the two layers. The model is based on moderate rotations theory, which is an extension of linear elasticity that accounts for moderate-to-large deflections and rotations. We derive explicit expressions that link the material properties of the two layers to the overall behavior.

To validate the framework, we consider free-standing bi-layer beams subjected to two types of boundary loadings: (1) applying a voltage across the two layers such that the bi-layer beam is under an electric field and (2) electric excitation of one layer while the second layer remains passive. The model agrees with FE simulations, which highlight its validity and merit. Interestingly, our findings show that the activation of a single layer leads to a larger bending than the if both layers are subjected to an electric field. This result is explained as follows: the electric field aims to stretch the layer on which it acts. Applying an electric field to the two layers leads to an overall extension, and bending is obtained because of the difference in the amount of stretching. In the case of a single layer activation, the passive layer is non-responsive and therefore enables larger bending. We also show that in free-standing beams, the bending direction is given by the difference $\varepsilon_b Y_b - \varepsilon_t Y_t$.

With an eye towards applications, we continue by investigating the performance of bi-layers in weight lifting actuators and soft grippers. To this end, we consider three commonly employed DEs, namely VHB 4910, Elastosil RT 625, and Fluorosilicone 730, and simulate the response of bi-layers with different material compositions. We show that the actuators are capable of lifting small weights, and the lifting capabilities are improved when only one layer is activated. In the case of grippers, these are typically anchored to a base and should be treated as cantilevered beams. Interestingly, we find that the bending direction under these boundary conditions is determined by the difference $\varepsilon_t Y_t - \varepsilon_b Y_b$. Once again, our simulations show that the activation of a single layer yield larger deflections at lower voltages.

From a practical viewpoint, the application of the proposed framework requires careful consideration of the dimensions of the DE. Consider a DE film with the length L, width t, and thickness d. Commonly, DE films characterized by $L, t \gg d$ are used (i.e. the two planar dimensions are significantly larger than the thickness), typically with square or rectangular dimensions. In the presence of passive constraints, electric excitation leads to the bending of the film along two directions into a concave or a convex shape (Shian et al., 2015; Su et al., 2020; Tutcuoglu and Majidi, 2014). The proposed model follows other works (Sikulskyi et al., 2022; Zhou et al., 2020; Chen et al., 2024) and considers slender DE beams in which $L \gg t, d$ (i.e. the length is much larger than the thickness and the width). Accordingly, one can treat the beam as a 1-D element. While this assumption does not capture transverse bending, it provides simple and useful approximations that enable one to program the response of DEs in the appropriate limit. It is underscored that the error in the final predictions of the response increases as one moves further away from the appropriate limit (i.e. in DEs with larger ratios t/d).

In conclusion, the findings from this work provide a fundamental understanding of the electro-mechanical response of bi-layer DE beams. The model sheds light on the relations between the electro-mechanical properties of the two layers and the resulting deformation field, and thereby allows one to optimize design in a variety of applications, including actuators and soft robotics.

CRediT authorship contribution statement

Karine Sacagiu: Writing – original draft, Validation, Investigation. **Silvia Monchetti:** Visualization, Software, Investigation. **Roberto Brighenti:** Writing – review & editing, Writing – original draft, Supervision, Methodology, Formal analysis. **Noy Cohen:** Writing – review & editing, Writing – original draft, Visualization, Supervision, Investigation, Formal analysis, Conceptualization.

Declaration of competing interest

The authors declare that they have no known competing financial interests or personal relationships that could have appeared to influence the work reported in this paper.

Appendix A. Supplementary data

Supplementary material related to this article can be found online at https://doi.org/10.1016/j.mechmat.2026.105626.

Data availability

Data will be made available on request.

References

Ahmed, S., Ounaies, Z., Frecker, M., 2014. Investigating the performance and properties of dielectric elastomer actuators as a potential means to actuate origami structures. Smart Mater. Struct. 23 (9), 094003.

Ask, A., Menzel, A., Ristinmaa, M., 2012a. Electrostriction in electro-viscoelastic polymers. Mech. Mater. 50, 9–21.

Ask, A., Menzel, A., Ristinmaa, M., 2012b. Phenomenological modeling of viscous electrostrictive polymers. Int. J. Non-Linear Mech. 47 (2), 156–165.

Aziz, S., M. Spinks, G., 2020. Torsional artificial muscles. Mater. Horizons 7 (3), 667–693.

Bar-Cohen, Y., 2001. EAP history, current status, and infrastructure. In: Bar-Cohen, Y. (Ed.), Electroactive Polymer (EAP) Actuators As Artificial Muscles. SPIE Press, Bellingham, WA, pp. 3–44.

Bazaev, K., Cohen, N., 2022. Electrically-induced twist in geometrically incompatible dielectric elastomer tubes. Int. J. Solids Struct. 250, 111707.

Bortot, E., Gei, M., 2015. Harvesting energy with load-driven dielectric elastomer annular membranes deforming out-of-plane. Extrem. Mech. Lett. 5, 62–73.

Bozlar, M., Punckt, C., Korkut, S., Zhu, J., Chiang Foo, C., Suo, Z., Aksay, I.A., 2012. Dielectric elastomer actuators with elastomeric electrodes. Appl. Phys. Lett. 101 (9), 091907.

Brighenti, R., Menzel, A., Vernerey, F.J., 2018. A physics-based micromechanical model for electroactive viscoelastic polymers. J. Intell. Mater. Syst. Struct. 29 (14), 2902–2918.

Cao, J., Lu, G., Shiju, E., Gao, Z., Zhao, T., Xia, W., 2021. Electrostatic model of dielectric elastomer generator based on finite element. Sci. Rep. 11.

Carpi, F., De Rossi, D.E., 2010. Electroactive polymer artificial muscles: An overview. WIT Trans. Ecol. Environ. 138, 353–364.

Chen, J., Qu, W., Ye, C., Zhao, Z., Wang, H., 2024. Nonlinear vibration and dynamic stability of dielectric sandwich micro-beams. Int. J. Mech. Sci. 262, 108738.

Cohen, N., 2017a. Enhancing the electro-mechanical response of stacked dielectric actuators. J. Elasticity 127 (1), 103–113.

Cohen, N., 2017b. Stacked dielectric tubes with electromechanically controlled radii. Int. J. Solids Struct. 108, 40–48.

Cohen, N., 2018. A generalized electro-elastic theory of polymer networks. J. Mech. Phys. Solids 110, 173–191.

Cohen, N., McMeeking, R.M., Begley, M.R., 2019. Modeling the non-linear elastic response of periodic lattice materials. Mech. Mater. 129, 159–168.

Cohen, N., Menzel, A., deBotton, G., 2016. Towards a physics-based multiscale modelling of the electro-mechanical coupling in electro-active polymers. Proc. R. Soc. Lond. A: Math. Phys. Eng. Sci. 472 (2186).

Cohen, N., Oren, S.S., deBotton, G., 2017. The evolution of the dielectric constant in various polymers subjected to uniaxial stretch. Extrem. Mech. Lett. 16, 1–5.

Croce, S., Neu, J., Moretti, G., Hubertus, J., Schultes, G., Rizzello, G., 2022. Finite element modeling and validation of a soft array of spatially coupled dielectric elastomer transducers. Smart Mater. Struct. 31 (8), 084001.

Dorfmann, A., Ogden, R.W., 2005. Nonlinear electroelasticity. Acta Mech. 174, 167–183.

Dorfmann, L., Ogden, R.W., 2023. The nonlinear theory of magnetoelasticity and the role of the Maxwell stress: A review. Proc. R. Soc. A 479 (2278), 20230592.

Duduta, M., Wood, R.J., Clarke, D.R., 2016. Multilayer dielectric elastomers for fast, programmable actuation without prestretch. Adv. Mater. 28 (36), 8058–8063.

Franke, M., Ehrenhofer, A., Lahiri, S., Henke, E.-F., Wallmersperger, T., Richter, A., 2020. Dielectric elastomer actuator driven soft robotic structures with bioinspired skeletal and muscular reinforcement. Front. Robot. AI 7, 510757.

Gei, M., Colonnelli, S., Springhetti, R., 2014. The role of electrostriction on the stability of dielectric elastomer actuators. Int. J. Solids Struct. 51 (3), 848–860.

Gei, M., Springhetti, R., Bortot, E., 2013. Performance of soft dielectric laminated composites. Smart Mater. Struct. 22 (10), 104014.

Guo, Y., Li, L., Zhang, D., Liao, W.-H., 2025. Dynamic modeling and analysis for dielectric elastomer tube actuators. Int. J. Mech. Sci. 288, 109994.

Guo, Y., Liu, L., Liu, Y., Leng, J., 2021. Review of dielectric elastomer actuators and their applications in soft robots. Adv. Intell. Syst. 3 (10), 2000282.

Hajiesmaili, E., Clarke, D.R., 2021. Dielectric elastomer actuators. J. Appl. Phys. 129 (15), 151102.

Hanuhov, T., Brighenti, R., Cohen, N., 2024. Energy harvesting with dielectric elastomer tubes: active and (responsive materials-based) passive approaches. Smart Mater. Struct. 33 (5), 055004.

Hanuhov, T., Cohen, N., 2022. Thermally induced deformations in multi-layered polymeric struts. Int. J. Mech. Sci. 215, 106959.

He, L., Lou, J., Du, J., Wang, J., 2017. Finite bending of a dielectric elastomer actuator and pre-stretch effects. Int. J. Mech. Sci. 122, 120–128.

Henann, D.L., Chester, S.A., Bertoldi, K., 2013. Modeling of dielectric elastomers: Design of actuators and energy harvesting devices. J. Mech. Phys. Solids 61 (10), 2047–2066.

Jamali, A., Knoerlein, R., Mishra, D.B., Sheikholeslami, S.A., Woias, P., Goldschmidt-boeing, F., 2024. Soft gripping fingers made of multi-stacked dielectric elastomer actuators with backbone strategy. 9, (8),

Khurana, A., Joglekar, M.M., Motzki, P., Seelecke, S., 2024. Compliant frame geometry for DEMES-based gripper and flapping wing actuators: A comprehensive design study. Int. J. Solids Struct. 302, 112969.

Khurana, A., Kumar, A., Raut, S.K., Sharma, A.K., Joglekar, M.M., 2021a. Effect of viscoelasticity on the nonlinear dynamic behavior of dielectric elastomer minimum energy structures. Int. J. Solids Struct. 208–209, 141–153.

Khurana, A., Sharma, A.K., Joglekar, M.M., 2021b. Nonlinear oscillations of electrically driven aniso-visco-hyperelastic dielectric elastomer minimum energy structures. Nonlinear Dynam. 104 (3), 1991–2013.

Kofod, G., 2008. The static actuation of dielectric elastomer actuators: how does pre-stretch improve actuation? J. Phys. D: Appl. Phys. 41 (21), 215405.

Kofod, G., Sommer-Larsen, P., 2005. Silicone dielectric elastomer actuators: Finite-elasticity model of actuation. Sensors Actuators A: Phys. 122 (2), 273–283.

Kofod, G., Sommer-Larsen, P., Kornbluh, R., Pelrine, R., 2003. Actuation response of polyacrylate dielectric elastomers. J. Intell. Mater. Syst. Struct. 14, 787–793.

Kornbluh, R., Pelrine, R., 2008. Chapter 4 high-performance acrylic and silicone elastomers. In: Dielectric Elastomers As Electromechanical Transducers.

Kovacs, G., Düring, L., 2009. Contractive tension force stack actuator based on soft dielectric EAP. In: SPIE Smart Structures and Materials+ Nondestructive Evaluation and Health Monitoring. International Society for Optics and Photonics, 72870A–72870A.

Kovacs, G., Düring, L., Michel, S., Terrasi, G., 2009. Stacked dielectric elastomer actuator for tensile force transmission. Sensors Actuators A: Phys. 155 (2), 299–307.

Kumar, D., Arya, K., Sarangi, S., 2019. Modeling of a pre-stretched dielectric elastomer : A second law of thermodynamics-based approach. J. Phys.: Conf. Ser. 1276 (1), 012047.

Kumar, D., Sarangi, S., 2020. Pre-stretching effect modeling of a dielectric elastomer under the electrical loading condition. Mater. Today: Proc. 24, 290–297.

Li, B., Chen, H., Qiang, J., Hu, S., Zhu, Z., Wang, Y., 2011. Effect of mechanical pre-stretch on the stabilization of dielectric elastomer actuation. J. Phys. D: Appl. Phys. 44 (15), 155301.

Liu, L., Li, J., Liu, Y., Leng, J., Zhao, J., Zhao, J., 2015. Electric field induced variation of temperature and entropy in dielectric elastomers. J. Mech. Sci. Technol. 29 (1), 109–114.

Liu, C.-H., Lin, P.-W., Chen, J.-A., Lee, Y.-T., Chang, Y.-M., 2017. Exploiting stretchable metallic springs as compliant electrodes for cylindrical dielectric elastomer actuators (DEAs). 8, (11),

Lotz, P., Matysek, M., Schlaak, H.F., 2011. Fabrication and application of miniaturized dielectric elastomer stack actuators. Mechatronics, IEEE/ASME Trans. on 16 (1), 58–66.

Madsen, F.B., Daugaard, A.E., Hvilsted, S., Skov, A.L., 2016. The current state of silicone-based dielectric elastomer transducers. Macromol. Rapid Commun. 37 (5), 378–413.

McKay, T., O'Brien, B., Calius, E., Anderson, L., 2010. An integrated, self-priming dielectric elastomer generator. Appl. Phys. Lett. 97, 062911.

McMeeking, R.M., Landis, C.M., Jimenez, S.M.A., 2007. A principle of virtual work for combined electrostatic and mechanical loading of materials. Int. J. Nonlinear Mech. 42 (6), 831–838.

Nejati, A., Mohammadi, H., 2023. A finite element modeling for anisotropic dielectric elastomer energy harvesters with inhomogeneous displacement fields. Eur. J. Mech. A Solids 102, 105086.

Pelrine, R., Kornbluh, R., Joseph, J., Heydt, R., Pei, Q., Chiba, S., 2000a. High-field deformation of elastomeric dielectrics for actuators. Mater. Sci. Eng.: C 11 (2), 89–100.

Pelrine, R., Kornbluh, R., Pei, Q., Joseph, J., 2000b. High-speed electrically actuated elastomers with strain greater than 100%. Science 287 (5454), 836–839.

Shian, S., Bertoldi, K., Clarke, D.R., 2015. Dielectric elastomer based "Grippers" for soft robotics. Adv. Mater. 27 (43), 6814–6819.

Shmuel, G., 2015. Manipulating torsional motions of soft dielectric tubes. J. Appl. Phys. 117 (17), 174902.

Sikulskyi, S., Ren, Z., Mekonnen, D.T., Holyoak, A., Srinivasaraghavan Govindarajan, R., Kim, D., 2022. Additively manufactured unimorph dielectric elastomer actuators: Design, materials, and fabrication. Front. Robot. AI 9, 1034914.

Springhetti, R., Bortot, E., deBotton, G., Gei, M., 2014. Optimal energy-harvesting cycles for load-driven dielectric generators in plane strain. IMA J. Appl. Math. 79 (5), 929–946.

Su, Y.P., Chen, W.Q., Destrade, M., 2019. Tuning the pull-in instability of soft dielectric elastomers through loading protocols. Int. J. Non-Linear Mech. 113, 62–66.

Su, Y., Wu, B., Chen, W., Destrade, M., 2020. Pattern evolution in bending dielectric-elastomeric bilayers. J. Mech. Phys. Solids 136, 103670.

Suo, Z., Zhao, X., Greene, W.H., 2008. A nonlinear field theory of deformable dielectrics. J. Mech. Phys. Solids 56 (2), 467–486.

Thongking, W., Wiranata, A., Minaminosono, A., Mao, Z., Maeda, S., 2021. Soft robotic gripper based on multi-layers of dielectric elastomer actuators:. J. Robot. Mechatronics 33 (4), 968–974.

Tutcuoglu, A., Majidi, C., 2014. Energy harvesting with stacked dielectric elastomer transducers: Nonlinear theory, optimization, and linearized scaling law. Appl. Phys. Lett. 105 (24).

Wang, Y., Ma, X., Jiang, Y., Zang, W., Cao, P., Tian, M., Ning, N., Zhang, L., 2022. Dielectric elastomer actuators for artificial muscles: A comprehensive review of soft robot explorations. Resour. Chem. Mater. 1 (3), 308–324.

Wissler, M., Mazza, E., 2005. Modeling and simulation of dielectric elastomer actuators. Smart Mater. Struct. 14 (6), 1396.

Wissman, J., Finkenauer, L., Deseri, L., Majidi, C., 2014. Saddle-like deformation in a dielectric elastomer actuator embedded with liquid-phase gallium-indium electrodes. J. Appl. Phys. 116 (14), 144905.

Xiao, Y., Mao, J., Shan, Y., Yang, T., Chen, Z., Zhou, F., He, J., Shen, Y., Zhao, J., Li, T., Luo, Y., 2020. Anisotropic electroactive elastomer for highly maneuverable soft robotics. Nanoscale 12 (14), 7514–7521.

Xu, C., Faul, C.F.J., Taghavi, M., Rossiter, J., 2023. Electric field-driven dielectrophoretic elastomer actuators. Adv. Funct. Mater. 33 (13), 2208943.

Yang, C., Wang, W., Yao, C., Xie, R., Ju, X.-J., Liu, Z., Chu, L.-Y., 2015. Hydrogel walkers with electro-driven motility for cargo transport. Sci. Rep. 5 (1), 13622.

Yoder, Z., Rumley, E.H., Schmidt, I., Rothemund, P., Keplinger, C., 2024. Hexagonal electrohydraulic modules for rapidly reconfigurable high-speed robots. Sci. Robot. 9 (94), eadl3546.

Zhang, C., Wei, W., Sun, H., Zhu, Q., 2021. Study on the properties of different dielectric elastomers applying to actuators. Sensors Actuators A: Phys. 329, 112806.

Zhang, Q., Yu, W., Zhao, J., Meng, C., Guo, S., 2025. A review of the applications and challenges of dielectric elastomer actuators in soft robotics. 13, (2),

Zhou, F., Yang, X., Xiao, Y., Zhu, Z., Li, T., Xu, Z., 2020. Electromechanical analysis and simplified modeling of dielectric elastomer multilayer bending actuator. AIP Adv. 10 (5), 055003.

Zurlo, G., Destrade, M., DeTommasi, D., Puglisi, G., 2017. Catastrophic thinning of dielectric elastomers. Phys. Rev. Lett. 118, 078001.